Optical second harmonic generation studies of ultrathin high-*k* dielectric stacks

V. Fomenko
JILA, University of Colorado, Boulder, Colorado 80309

E. P. Gusev
IBM T.J. Watson Research Center, and Semiconductor Research and Development Center (SRDC), Yorktown Heights, New York 10598

E. Borguet
Department of Chemistry, Temple University, Philadelphia, Pennsylvania 19122

(Received 24 March 2004; accepted 17 December 2004; published online 11 April 2005)

We report an investigation of charge transfer in high-*k* dielectric stacks on Si by second harmonic generation (SHG). Ultrathin (2–6 nm) films of HfO_2, ZrO_2, and Al_2O_3 grown on Si surfaces by atomic layer deposition were investigated and compared to conventional SiO_2-based gate dielectrics. From the SHG rotational anisotropy (SHG-RA) of Si-(high-*k*) and $Si-SiO_2$ systems, optical roughness of the films was found to increase in the following order: SiO_2, Al_2O_3, and (ZrO_2 and HfO_2). The optical roughness is regarded as a quantity describing the nonuniformity in the distribution of interfacial defects capable of charge trapping. Time dependent second harmonic generation (TD-SHG) measurements were carried out to understand charge trapping and detrapping dynamics and trapped charge densities. Relative comparison of the four dielectrics revealed that Al_2O_3 films have the highest densities of trapped and fixed charge while silicon oxides exhibited less charge trapping, consistent with electrical measurements performed on similar structures. In contrast to SiO_2 films, detrapping was significantly suppressed in the high-*k* films due to significantly reduced leakage currents. We also observed ambient effects in charge trapping at the dielectric/air(vacuum) interface that could be significantly reduced by covering the dielectric film with a thin (semitransparent) metal (aluminum) overlayer. © *2005 American Institute of Physics*. [DOI: 10.1063/1.1861146]

I. INTRODUCTION

The scaling of integrated-circuit technology continues to be critical for the Si-based microelectronics industry in order to increase the functionality of microelectronic devices.[1,2] Scaling issues are particularly important for the advancement of the dominant Si technologies, such as complementary metal-oxide-semiconductor (CMOS) devices and dynamic random-access memory (DRAM).[1] One important element of these technologies is found in the metal-oxide-semiconductor field-effect transistor device (MOSFET). The key to the performance of these devices is the gate dielectric. As conventional SiO_2-based gate dielectrics approach the fundamental limit of their scaling (at ~1 nm), research on higher relative permittivity (high-*k*) dielectrics becomes increasingly important.[1–12]

The success of an alternative high-*k* dielectric is contingent upon several issues including low leakage current and high capacitance (drive current).[1] Other important electrical considerations include charge trapping in the dielectric and the effect of the dielectric on the channel carrier mobility. The impact of charge trapping on device performance is twofold. First, it brings about drive current reduction due to electrostatic interactions with trapped charges. Second, it causes threshold voltage instabilities over device operation time, which is an important dielectric reliability issue. Some experiments on poly-Si-gated field-effect transistors with Al_2O_3 or HfO_2 dielectrics have shown that the high-*k* dielectrics, compared to SiO_2, are several orders of magnitude more likely to trap charges leading to unacceptable threshold shifts (see Ref. 7 and Refs. 19,20 therein).

Characterization of charge traps in the Si/SiO_2 system is usually accomplished with electrical methods such as capacitance-voltage and current–voltage measurements.[13–15] Nondestructive, noncontact, *in situ* optical techniques, such as second harmonic generation, can offer additional advantages and insights in oxide trap characterization. SHG is a versatile probe of buried semiconductor interfaces that are difficult to probe by conventional spectroscopic methods.[16–19] SHG provides surface sensitivity and can be carried out *in situ*.[16–19] As an optical technique, SHG offers potential advantages of spatial, temporal and spectral resolution that are typically not available with conventional techniques. It is the purpose of this paper to demonstrate and develop SHG characterization of charge transfer in novel high-*k* dielectric films on Si. The paper is organized as follows. Following the experimental (sample preparation and characterization set-up description) section, we focus on the basics of SHG for interface characterization and specifically its application to high-*k* stacks. Then, we present data on SHG rotational anisotropy and interface roughness estimates. A significant part of the paper is devoted to time-dependent SHG measurements of charge trapping and detrapping. Fi-

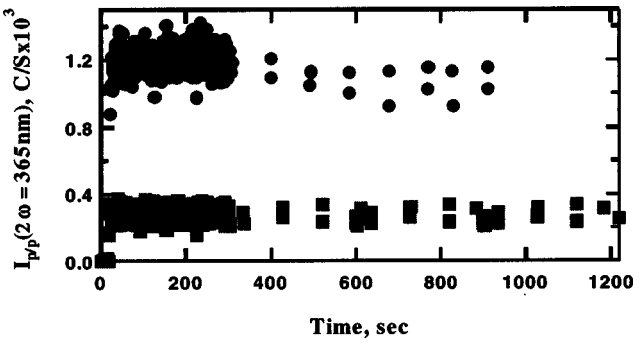

FIG. 1. *s*-polarized SHG from 2 nm SiO_2 on Si(100). The absence of TD-SHG confirms insensitivity of *s*-polarized SHG to EFISH. *n*-type Si, 24 Ω cm, λ_ω=730 nm, 10 kW/cm^2. •, *p*-in/*s*-out SHG; ■, *s*-in/*s*-out SHG.

nally, we discuss the effect of the ambient on charge trapping behavior.

II. EXPERIMENT

SHG measurements were conducted in both angular resolved (using SHG-RA) and time-dependent modes (using TD-SHG). TD-SHG experiments were carried out in ambient air by illuminating the sample with Ti:sapphire femtosecond oscillator fundamental light at 730 nm at an average irradiance of 10 kW/cm^2 and recording the SHG response as a function of illumination time. The samples were azimuthally oriented to a maximum of the rotational anisotropy pattern determined at low (4 kW/cm^2) power at 730 nm. Experiments were performed at 45° angle of incidence with 730 nm *p*-polarized input light and *p*-polarized second-harmonic. *p*-polarized SHG was used since it provides maximum sensitivity to interfacial charge buildup.[20] Photons were counted continuously in 0.5-s intervals. The postillumination recovery of the second harmonic response of the sample was followed by unblocking the laser and sampling the SHG for ~1 sec, at discrete intervals.

Charge trapping and detrapping in the dielectric/Si(100) stacks reveals itself through time-dependent SHG. The observed TD-SHG is attributed to the electric-field-induced second harmonic generation (EFISH), caused by photogenerated charges trapped in the dielectric.[21–23] A simple model, treating the interface as a uniformly-charged plane, was used as a first approximation to estimate the relative charge trap densities in the high-*k* dielectrics. We use the charge-plane approximation since the thickness of the high-*k* material was small (~2–6 nm), much less than the lateral SHG probe dimensions (at most 30 μm) and extent of the space charge region (~600 nm) and because the high-*k* dielectric was located outside of the semiconductor bulk.

High-*k* dielectrics were grown by atomic layer deposition (ALD) at 300 °C on moderately-doped (0.6–1.5 Ω cm for Al_2O_3 and ZrO_2 and 8-24 Ω cm for HfO_2) *n*-Si(100). Before HfO_2, ZrO_2, and Al_2O_3 depositions, a thin (~1 nm) silicon oxynitride layer was thermally pregrown on Si which is known to improve high-*k* nucleation during the ALD process. More details on ALD processes and physical characterization of ALD deposited high-*k* films can be found elsewhere.[24,25] The high-*k* films were benchmarked against conventional SiO_2-based films of similar thickness (1–3 nm) that were either thermally grown or deposited by chemical vapor deposition on Si. A native oxide on Si was used as the thinnest standard in our measurements. The high-*k* oxides described above were selected because of their technological relevance in modern semiconductor industry—the oxides of Al, Hf, and Zr are the most likely candidates to replace SiO_2 in future semiconductor devices.

III. RESULTS AND DISCUSSION

The interfacial charge buildup manifests itself through the electric-field induced second harmonic contribution to the SHG signal. The nonlinear polarization governing the EFISH contribution to SHG can be expressed as

$$P^{\mathrm{EFISH}}(2\omega) \propto \chi^{(3)}(2\omega;\omega;\omega;0):E(\omega)E(\omega)E_{\mathrm{dc}}, \tag{1}$$

where $E(\omega)$ is the amplitude of the laser light fundamental field and the E_{dc} is the amplitude of the constant (dc) electric field in the semiconductor due to interface charging.[21,26,27] The $\chi^{(3)}$ tensor for cubic crystals has only three nonequivalent components, Eq. (2):[26]

$$\begin{aligned}
&\chi_1^{(3)} \equiv \chi_{xxxx} = \chi_{yyyy} = \chi_{zzzz},\\
&\chi_2^{(3)} \equiv \chi_{xyyx} = \chi_{yxxy} = \chi_{xzzx} = \chi_{yzzy} = \chi_{zxxz} = \chi_{zyyz},\\
&\chi_3^{(3)} \equiv \chi_{xyxy} = \chi_{xxyy} = \chi_{yyxx} = \chi_{yxyx} = \chi_{xyyx} = \chi_{xxzz} = \chi_{xzxz}\\
&\quad = \chi_{yyzz} = \chi_{yzyz}.
\end{aligned} \tag{2}$$

Assuming that the charge buildup leads to E_{dc} perpendicular ($E_{\mathrm{dc}}=E_{\mathrm{dc}}^Z$) to the interface and considering the nonzero elements of the $\chi^{(3)}$ tensor at the (100) interface, the following expressions for the distinct polarization components for the dielectric/Si(100) stacks can be obtained:

$$\begin{aligned}
P_{pp}^{\mathrm{EFISH}}(2\omega) = [&\chi_1^{(3)} \sin^2\theta + \chi_3^{(3)} \cos^2\theta\\
&+ 2\chi_2^{(3)} \cos\theta \sin\theta]E_{\mathrm{dc}}^Z(E(\omega))^2,
\end{aligned} \tag{3}$$

$$P_{sp}^{\mathrm{EFISH}}(2\omega) = [\chi_3^{(3)}]E_{\mathrm{dc}}^Z(E(\omega))^2, \tag{4}$$

$$P_{ss}^{\mathrm{EFISH}}(2\omega) = P_{ps}^{\mathrm{EFISH}}(2\omega) \equiv 0, \tag{5}$$

where θ is the angle of incidence. Thus, *s*-polarized SHG should not depend on interfacial charging. This conclusion was verified in the experiments with *s*-out SHG, Fig. 1. The

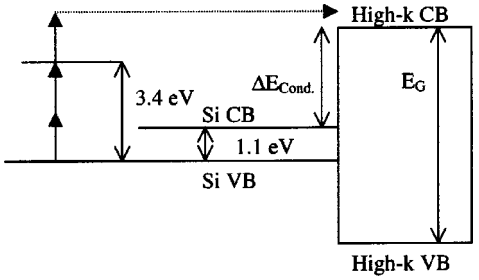

FIG. 2. The band offset, ΔE_{Cond}, of a high-*k* dielectric on Si. Multiphoton path of electron injection into high-*k* dielectric is shown. Two photon resonance at 3.4 eV, the direct gap of Si, increases the efficiency of the process.

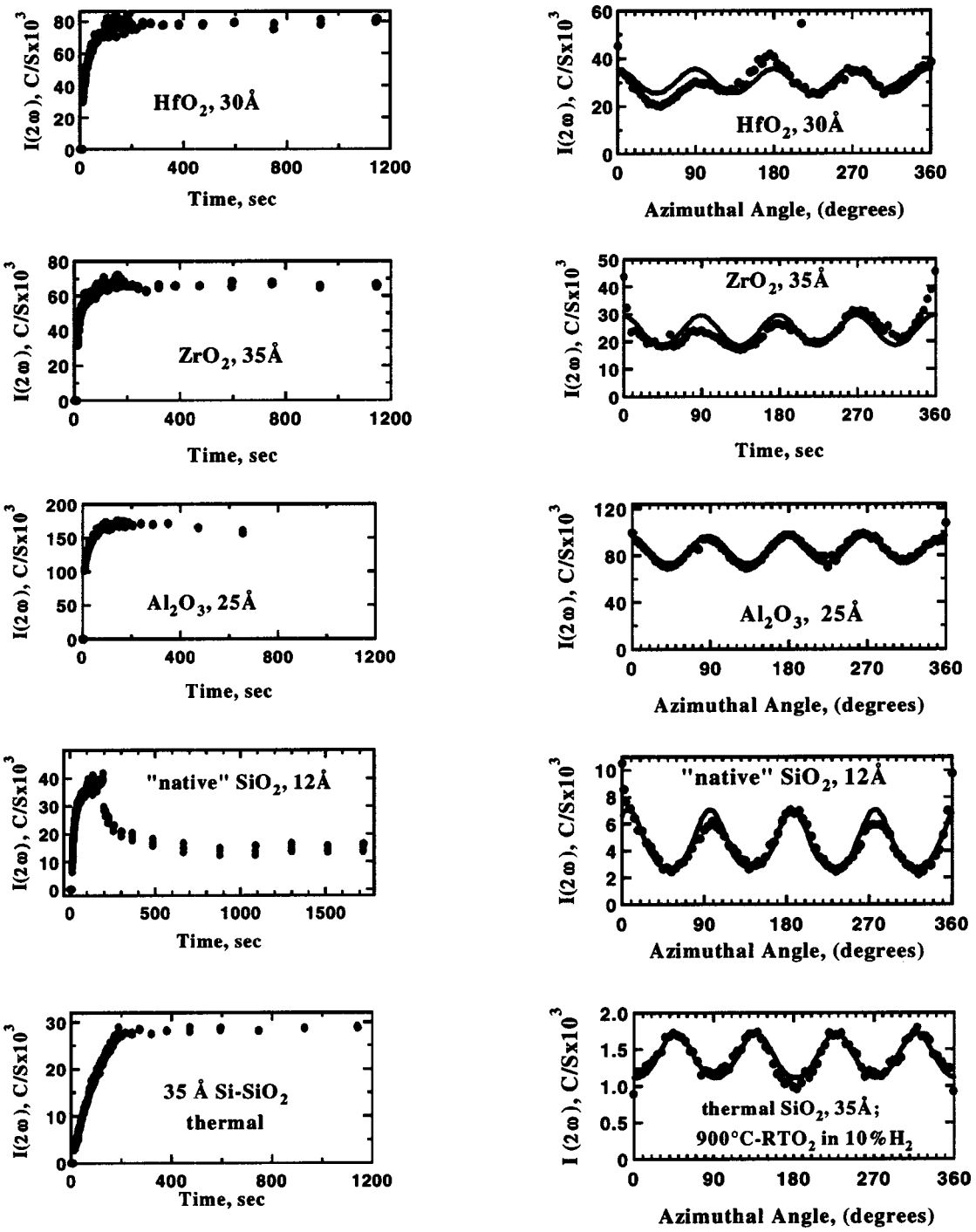

FIG. 3. TD-SHG and SHG-RA data on Si(100) with high-k and SiO_2 dielectrics.

lack of TD-SHG confirms that *s*-polarized SHG is insensitive to interfacial charging.

The injection of charge in the high-k dielectric occurs through a multiphoton process,[21] as shown in Fig. 2, and is resonantly enhanced at the point of two-photon resonance with the E_1 critical point in Si.

SHG studies were performed to characterize charge trapping density of Si(100) with the following high-k dielectrics: Al_2O_3, ZrO_2, HfO_2. TD-SHG on Si(100) with various high-k dielectrics is presented in Fig. 3 along with rotational anisotropy scans taken at 730 nm.

Note that thermal oxide SHG-RA starts "low" whereas all the others start "high." This may reflect the fact that the thermal oxide is "better" in terms of having less initial oxide defects. Thermal oxides, grown at elevated temperatures and in the presence of H_2 are likely to yield interfaces with less defects and therefore, charge traps compared to native oxides, due to two mechanisms: (a) elevated temperatures that "anneal" the interface and (b) the action of H_2. One can speculate that "native" oxide should have a higher density of interfacial defects, hence charge traps, hence initial fixed oxide charge as compared to thermal oxides. In this respect, "native" oxide stays somewhere between thermal oxides and high-k dielectrics in terms of oxide trap density. High-k di-

electrics have more charge traps and therefore, are likely to accumulate more initial oxide charge. It is noteworthy that high-*k* dielectrics and "native" oxide have the same initial phase— they start "high" in SHG-RA.

A. Estimates of interface "roughness"

SHG-RA has been postulated to be sensitive to surface roughness.[22,28,29] SHG-RA from the Si(100) surface can be described by the functional form

$$I_{2\omega}^{(100)}(\phi) = |A + B\cos(4\phi)|^2, \tag{6}$$

where A and B are complex constants and ϕ is the azimuthal angle of rotation measured with respect to the $\langle 010 \rangle$ direction of the (100) surface.[30] For ideal (100) surfaces, A arises from both bulk (quadrupole) and surface (dipole/multipole) contributions while B reflects the bulk quadrupole contribution alone. Therefore, since the (100) interface only contributes to A, it was suggested that the ratio $|A/B|$ provides sensitivity to interface roughness.[28,29]

The sensitivity of SHG to surface roughness was suggested in a series of etching experiments, when the Si(100) interface was roughened in repeated cycles of HF oxide stripping. The SHG-RA $|A/B|$ ratio went down exponentially as the surface roughness, characterized by AFM measurements, increased.[28] Interestingly, the magnitude of s-polarized SHG patterns, that can be attributed solely to the bulk response of Si(100), did not change with AFM roughness.[28] A similar qualitative correlation was found between the $|A/B|$ ratio and the surface roughness in a combined SHG/x-ray scattering study of $Si(100)-SiO_2$ with thermal SiO_2 of various thickness, grown after HF-stripping of native oxide.[29] The difference was that in the SHG/x-ray study the $|A/B|$ ratio decreased linearly (not exponentially, as in Ref. 28) as the interface roughness determined by x-ray scattering increased.[29] The range of interface roughness measured in the SHG-x-ray study was much smaller than that measured in the SHG/AFM study, thus the authors concluded that the linear and exponential dependencies were not inconsistent.[29]

However, in a study of plasma etching of thermally-grown SiO_2 on Si(100), SHG-RA patterns were found to "deteriorate" with oxide thinning.[22] "Deterioration" exhibited itself through a reduction of the anisotropic contribution in the SHG-RA signal, i.e. the ratio $|A/B|$ increased with the etching time. As the thermal oxide layer was not completely removed in the plasma etch experiments, the $Si-SiO_2$ interface was most likely unaffected. Remarkably, after a complete oxide removal, the $|A/B|$ ratio again became close to the value determined on oxide prior to the plasma etch.[22] The "deterioration" of SHG-RA was attributed to the creation and non-uniform distribution of defects capable of charge trapping in the oxide layer.[22] Clearly, this study suggests that the $|A/B|$ ratio can be affected by factors other than interface topological roughness.

SHG-RA is sensitive to changes in the local environment of interfacial atoms such as surface defects or charge traps.[29] SHG "roughness" may, therefore, reflect factors other than a pure physical morphology of the interface.[22,29] In particular, SHG, unlike AFM, averages the signal over the spot-size area (on the order of 30 μm) and is sensitive, unlike x-ray or ion scattering, to local electronic defects, like dangling bonds,[29] charge traps,[21] etc.

Since no significant differences were reported in the high-resolution transmission electron microscopy analysis of the high-*k* samples studied in this work, we speculate that the SHG-RA fluctuations may reflect the non-uniform lateral distribution of charge traps in the high-*k* oxides. The EFISH contribution to SHG fields from the nonuniformly-distributed high-*k* oxide traps differs at each azimuthal position causing "randomness" in the SHG-RA signal. With this picture in mind, we propose a novel method of characterizing SHG surface "roughness." The charge trapping sites can alter the local response of the interface through the electric-field induced second harmonic contribution to the SHG signal.[26] The $|A/B|$ ratio may vary with azimuthal angle and thus should be considered at various azimuths. The symmetry properties of the EFISH response are governed by a cubic susceptibility forth-rank tensor, $\chi^{(3)}$, whose symmetry properties have been described elsewhere.[26,30,31] The EFISH contributes both to the isotropic, A, and anisotropic, B, response of the (100) surface.[26,30,31]

Based on the second harmonic generation rotational anisotropy (SHG-RA) scans, presented in Fig. 3, an effective roughness of the interface can be estimated. Rather than using the $|A/B|$ ratio, we propose to characterize the interface SHG "roughness" by another parameter—the Δ^2 factor,

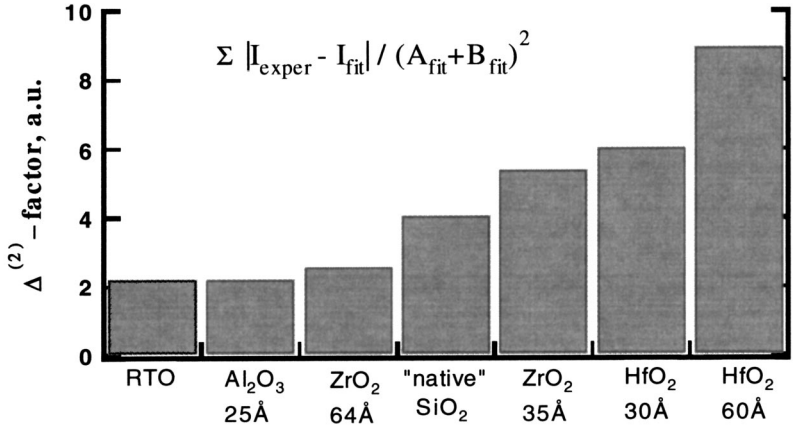

FIG. 4. SHG "roughness" of various high-*k* dielectrics on Si(100), described by Eq. (7).

which is a normalized sum of the squared differences between the experimental signal and a fit by Eq. (6), normalized by a max of the fit curve value:

$$\Delta^2 = \frac{\sum |I_{\exp}(\phi) - |A + B\cos(4\omega)|^2|}{(A+B)^2}, \tag{7}$$

where A and B are fit constants in Eq. (6). The greater the Δ^2 parameter, the greater the lateral variation in charge trap distribution. This analysis is presented below in Fig. 4 suggesting that, on the relative scale, the $Al_2O_3/SiO_2/Si$ stack shows the most uniform distribution of oxide charge traps as characterized by the Δ^2 factor of Eq. (7). This agrees qualitatively with superior uniformity of ALD-grown Al_2O_3 films (of all known ALD oxide processes). The lower values of Δ^2 for the thicker ZrO_2 suggests that the stack becomes "SHG-smooth" with increasing oxide thickness. Similar thickness dependence was observed for SiO_2 films earlier.[22,29,32]

B. Time-dependent SHG study

A very striking feature of the TD-SHG from the samples with alternative dielectrics, as opposed to TD-SHG on Si(100) with a native SiO_2, (p-Si-SiO2, 9–18 Ω cm) is the absence of TD-SHG signal recovery. This effect is very similar to TD-SHG on Si(100) with thermal SiO_2 with different thickness', where signal recovery becomes very slow for films thicker than ~3 nm, see Fig. 3.

We suggest that the reason for this very slow recovery stage of the TD-SHG on high-k dielectrics is the same as in thicker thermal SiO_2: photoexcited "hot" electrons are thermalized and get trapped in the bulk dielectric and at the dielectric/ambient interface. Detrapping presumably shuts off due to the reduced tunneling efficiency of "cold" trapped electrons back to Si that depends exponentially on the dielectric thickness.[33] Since gate leakage (due to tunneling) is known to be orders of magnitude lower (for comparable thickness) in high-k films compared to SiO_2 dielectrics extremely slow, TD-SHG signal recovery in such samples is not unreasonable extremely slow as a result.[24,34]

The magnitude of the initial, quiescent TD-SHG depends on the particular high-k dielectric, Fig. 3. We suggest that the difference in the oxide charge in the high-k dielectrics is responsible for the difference in the quiescent TD-SHG. The magnitude of TD-SHG achieved after the continuous laser irradiation is also different. The quiescent SHG can provide an estimate of the relative density of the fixed oxide charge in the high-k dielectrics. Assuming that TD-SHG contribution to SHG is described by Eq. (1), one can suggest that the density of interfacial charges, σ, is related to the magnitude of SHG signal in the following manner:

$$I(2\omega) \propto C\left|\chi^{(2)}_{\text{eff}} + \chi^{(3)}_{\text{eff}}{:}\sigma\right|^2, \tag{8}$$

where σ determines the static electric field E_{dc} of Eq. (1). As discussed by Aktsipetrov *et al.*, the polarization that provides the EFISH contribution to the second harmonic response is related to the integral of the dc electric field in Si as shown below[26]

$$P^{\text{EFISH}}_{pp}(2\omega) = C\int_0^\infty E_{\text{dc}}(z)\exp(i\Phi z)dz. \tag{9}$$

Here, C and Φ are complex-valued constants depending on the dielectric constants of Si at the fundamental and second harmonic frequencies, the reflection geometry and the values of the $\chi^{(3)}$ tensor elements of Si. $E_{\text{dc}}(z)$ is the spatial distribution of the static electric field in the Si space-charge region. The maximum effective thickness probed at 730 nm fundamental by SHG is determined by[35]

$$l^{\text{eff}}_{2\omega} \cong \frac{\lambda_\omega}{2(n_\omega + n_{2\omega})} \approx 36 \text{ nm}, \tag{10}$$

which is small compared to the space-charge region (~600 nm)—the extent of spatial variations of the static electric field in moderately-doped Si.[13] Since the region probed is thin compared the space-charge region, we used a simplified model of the probe region as a parallel-plate capacitor in which the magnitude of the electric field between the plates is proportional to the density of charges on the plates and is constant over the probe depth. Hence, $E_{\text{dc}}(z)$ can be taken outside of the integration sign in Eq. (9). By Gauss' theorem, $E_{\text{dc}}(z)$ is proportional to the density of the interfacial fixed charges, σ. Thus we can use Eq. (8) to evaluate the relative density of fixed charges, both in the bulk traps and in the interface traps, at various interfaces. We assume that at time $t=0$, most the traps are empty and the

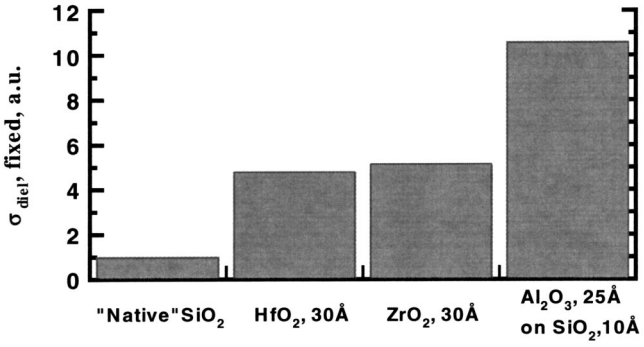

FIG. 5. Relative densities of fixed oxide charge at high-k dielectrics, evaluated by TD-SHG. Fixed oxide charge densities, are relative to that on the "native" oxide.

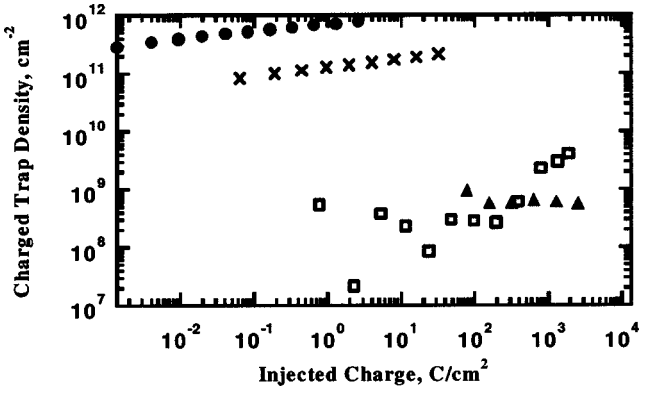

FIG. 6. Charge trap densities in high-k and SiO_xN_y dielectrics deduced from capacitance–voltage measurements. Indicated thickness is electrical equivalent oxide thickness (EOT), normalized to the dielectric constant of SiO_2. □, *in situ* deposited oxinitride stack (EOT=2.1); ▲, *ex situ* deposited oxinitride stack (EOT=2.1); ×, ALD HfO_2 (EOT=1.6); •, ALD Al_2O_3 (EOT=1.9).

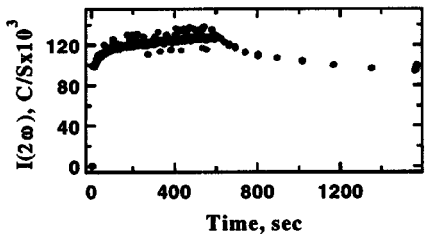

Si-(15 Å SiO_2)-(100Å Aluminum)

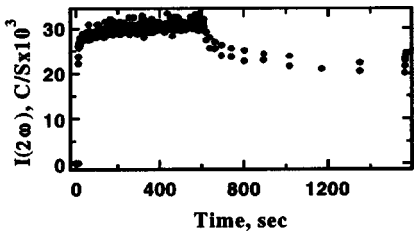

Si-(15 Å SiO_2)-(200Å Aluminum)

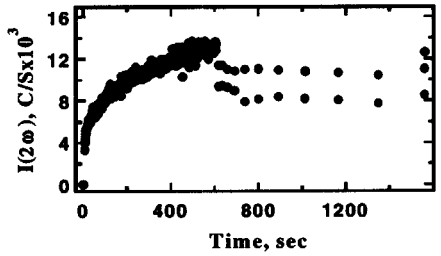

Si-(25Å Al_2O_3)-(100Å Aluminum)

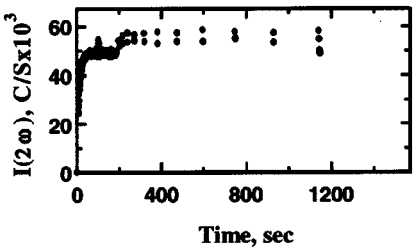

Si-(30Å HfO_2)-(100Å Aluminum)

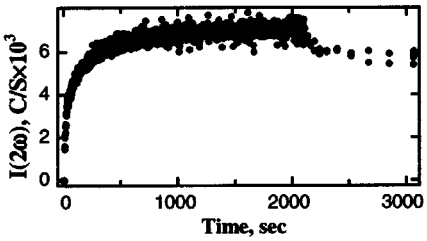

Si-(25Å Al_2O_3)-(200Å Aluminum)

FIG. 7. TD-SHG on Si with high-*k* dielectrics covered by aluminum films of various thickness.

interfacial oxide charge is mainly related to the dielectric fixed oxide charge, σ_{diel}. Given the fact that the magnitude of the quiescent TD-SHG on Si(100)-thermal-SiO_2 is at least an order of magnitude smaller than the quiescent TD-SHG on Si with high-*k* dielectrics, we can neglect the density of the fixed oxide charge in thermal-SiO_2 in comparison to that in Si-native oxide and Si-high-*k* dielectrics. We calibrate the magnitude of the fixed interfacial charge on high-*k* dielectrics using the Si-(thermal oxide) as a reference interface with negligible density of fixed oxide charge by the following method. First, we suggest that the initial, quiescent SHG on thermal-oxide-Si has negligible EFISH contribution and therefore can be expressed as

$$[I_{\text{ini}}^{\text{SiO}_2}(2\omega)]_{\text{thermal}} \propto C|\chi_{\text{eff}}^{(2)}|^2; |\chi_{\text{eff}}^{(2)}| \propto \sqrt{[I_{\text{ini}}^{\text{SiO}_2}(2\omega)]_{\text{thermal}}}. \tag{11}$$

The high-*k* dielectrics, however, are expected to have a considerable fixed charge and thus interfacial charge trap density, compared to SiO_2, and Si-oxynitride (interfacial charge trap densities in thermal oxides and Si-oxynitride are very similar), as evidenced by our independent electrical measurements, Fig. 6.

One should note that the stress condition used in the electrical measurements to inject charge into the dielectric are different from charge injection in the SHG experiments. Therefore, the comparison between charge trapping in electrical and SHG measurements is only qualitative at this point.

The effect of fixed oxide charge in high-*k* dielectrics on SHG can be expressed as

$$\sqrt{I_{\text{ini}}^{\text{high-}k}(2\omega)} \propto |\chi^{(2)} + \chi^{(3)}\sigma_{\text{fixed}}^{\text{high-}k}|. \tag{12}$$

Thus the fixed oxide charge density can be related to the SHG intensities as follows:

$$\sigma_{\text{fixed}}^{\text{high-}k} \propto \frac{\sqrt{I_{\text{ini}}^{\text{high-}k}(2\omega)} - \sqrt{[I_{\text{ini}}^{\text{SiO}_2}(2\omega)]_{\text{thermal}}}}{\sqrt{[I_{\text{ini}}^{\text{SiO}_2}(2\omega)]_{\text{thermal}}}} = \left|\frac{\chi^{(3)}}{\chi_{\text{eff}}^{(2)}}\sigma_{\text{fixed}}^{\text{high-}k}\right|. \tag{13}$$

Without invoking the explicit knowledge of the nonlinear susceptibility coefficients, the magnitude of the fixed oxide charge density on high-*k* dielectrics can be calibrated relative to the fixed oxide charge density on the Si-(native oxide) interface:

$$(\sigma_{\text{fixed}}^{\text{high-}k})_{\text{relative}} = \frac{\sigma_{\text{fixed}}^{\text{high-}k}}{\sigma_{\text{fixed}}^{\text{native}}} = \frac{\left|\frac{\chi^{(3)}}{\chi_{\text{eff}}^{(2)}}\sigma_{\text{fixed}}^{\text{high-}k}\right|}{\left|\frac{\chi^{(3)}}{\chi_{\text{eff}}^{(2)}}\sigma_{\text{fixed}}^{\text{native}}\right|} \propto \frac{\sqrt{I_{\text{ini}}^{\text{high-}k}(2\omega)} - \sqrt{[I_{\text{ini}}^{\text{SiO}_2}(2\omega)]_{\text{thermal}}}}{\sqrt{I_{\text{ini}}^{\text{native}}(2\omega)} - \sqrt{[I_{\text{ini}}^{\text{SiO}_2}(2\omega)]_{\text{thermal}}}}. \tag{14}$$

TABLE I. Relative charge trap densities ($\sigma_{trap}/\sigma_{fixed}$) in high-$k$ dielectrics (compared to SiO_2).

Sample	With 10 nm Al	With 20 nm Al	Average for 10 and 20 nm Al
2.5 nm Al_2O_3	0.99	1.2	1.1±0.1
3.0 nm HfO_2	0.42	…	0.42±0.1
1.5 nm SiO_2	0.13	0.17	0.15±0.2

The relative fixed oxide charges evaluated this way are shown in Fig. 5. The trend is similar to the electrical measurements where Al_2O_3 has shown trapped charge density higher than that of HfO_2 in the regime of low injected charge, Fig. 6. More details on charge trapping studies based on electrical (capacitance–voltage) measurements and electrical results for high-k gate stacks can be found elsewhere.[14,36]

TD-SHG can result from charge buildup in the oxide and at the oxide-ambient interface. The importance of ambient gas adsorption was shown in experiments with $Si-SiO_2$.[37] Our TD-SHG experiments (not shown here) on Si-oxynitride exhibited a dramatic increase in signal upon exposure of the N_2-purged chamber with Si-oxynitride to laboratory air ($T \sim 20\ ^\circ C$, RH$\sim$40%) supporting the importance of ambient gas adsorption.

To exclude the influence of the ambient gas adsorption and to simulate MOS devices, TD-SHG experiments were performed on Si-(high-k) dielectrics with aluminum films of 10 and 20 nm thickness, thermally evaporated on the high-k layer, Fig. 7. The aluminum was expected to prevent the adsorption of ambient gases on the surface and the associated interface charging. Thin 20 nm aluminum films on silicon are continuous (based on our scanning electron microscope images) and yet provide satisfactory optical transmission into bulk Si for SHG experiments.

Let us suppose that, in the sample with a thin Al overlayer, charge buildup is only due to bulk oxide traps. Then, assuming that the metal layer affects both the quiescent and the steady-state TD-SHG in the same manner, the following estimation can be suggested for the density of charge traps relative to fixed oxide charge in the high-k dielectrics:

$$\sigma_{REL} = \frac{\sigma_{trap}}{\sigma_{fixed}} \propto \frac{(\sqrt{I_{final}(2\omega)} - \sqrt{I_{ini}(2\omega)})_{On\ Aluminum}}{(\sqrt{I_{ini}(2\omega)})_{On\ Aluminum}}. \quad (15)$$

The results, shown in Table I, indicate that the high-k dielectric materials have higher density of charge traps compared to thermal $Si-SiO_2$.

IV. SUMMARY

SHG was used to probe the nonlinear optical response in high-k dielectric stacks on Si. The SHG-RA suggests a lateral inhomogeneity of the oxide in regard to fixed oxide charge and trap density. We propose a method for estimating the interfacial "roughness" of Si with high-k dielectrics. The "roughness" estimated by SHG signifies the distribution of charge traps in the oxide, rather than simply morphological roughness. For the dielectrics of comparable thickness, the interface "roughness" was found to decrease from HfO_2/Si to ZrO_2/Si to Al_2O_3/Si. Charge trapping and detrapping was studied by TD-SHG. We estimated relative densities of interfacial charge and fixed charge and found it to increase from SiO_2/Si to HfO_2/Si and ZrO_2/Si to Al_2O_3/Si. Detrapping in the high-k stacks is found to be very slow due to significantly reduced tunneling (leakage) currents.

ACKNOWLEDGEMENT

The authors acknowledge the generous support of the DOE, Office of Basic Energy Sciences.

[1] E. P. Gusev, *Ultrathin Oxide Films for Advanced Gate Dielectrics Applications. Current Progress and Future Challenges*, in Defects in SiO_2 and Related Dielectrics: Science and Technology, edited by G. Pacchioni, L. Skuja, and D. L. Griscom (Kluwer Academic, Dordrecht, 2000), pp. 557–579.
[2] R. M. Wallace and G. Wilk, MRS Bull. **27**, 192 (2002).
[3] T. Hori, *Dielectrics and MOS ULSIs* (Springer-Verlag, New York, 1997).
[4] D. G. Schlom and J. H. Haeni, MRS Bull. **27**, 198 (2002).
[5] J. Robertson, J. Vac. Sci. Technol. B **18**(3), 1785 (2000).
[6] D. A. Muller, T. Sorsch, S. Moccio, F. H. Baumann, K. Evans-Lutterodt, and G. Timp, Nature (London) **399**, 758 (1999).
[7] S. Guha, E. Gusev, M. Copel, L. Ragnarsson, and A. Buchanan, MRS Bull. **27**, 226 (2002).
[8] G. D. Wilk, R. M. Wallace, and J. M. Anthony, J. Appl. Phys. **89**, 5243 (2001).
[9] E. P. Gusev, M. Copel, E. Cartier, I. J. R. Baumvol, C. Krug, and M. A. Gribelyuk, Appl. Phys. Lett. **76**, 176 (2000).
[10] B. W. Busch, J. Kwo, M. Hong, J. P. Mannaerts, B. J. Sapjeta, W. H. Schulte, E. Garfunkel, and T. Gustafsson, Appl. Phys. Lett. **79**, 2447 (2000).
[11] M. Copel, M. Gribelyuk, and E. P. Gusev, Appl. Phys. Lett. **76**, 436 (2000).
[12] D. A. Neumayer and E. Cartier, J. Appl. Phys. **90**, 1801 (2001).
[13] S. A. Mitchell, T. R. Ward, D. D. M. Wayner, and G. P. Lopinski, J. Phys. Chem. B **106**, 9873 (2002).
[14] A. Kumar, T. H. Ning, M. V. Fischetti, and E. P. Gusev, J. Appl. Phys. **94**, 1728 (2003).
[15] E. P. Gusev, C. D'Emic, S. Zafar, and A. Kumar, Microelectron. Eng. **72**, 273 (2004).
[16] M. C. Downer, B. S. Mendoza, and V. I. Gavrilenko, Surf. Interface Anal. **31**, 966 (2001).
[17] G. Lüpke, Surf. Sci. Rep. **35**, 75 (1999).
[18] J. F. McGilp, Surf. Rev. Lett. **6**, 529 (1999).
[19] Y. R. Shen, Springer Ser. Surf. Sci. **2**, 77 (1985).
[20] V. Fomenko, C. Hurth, T. Ye, and E. Borguet, J. Appl. Phys. **91**, 4394 (2002).
[21] J. Bloch, J. G. Mihaychuk, and H. M. van Driel, Phys. Rev. Lett. **77**, 920 (1996).
[22] J. Fang, W. W. Heidbrink, and G. P. Li, J. Appl. Phys. **88**, 2641 (2000).
[23] V. Fomenko, J. F. Lami, and E. Borguet, Phys. Rev. B **63**, 121316 (2001).
[24] E. P. Gusev, E. Cartier, D. A. Buchanan, M. A. Gribelyuk, M. Copel, H. Okorn-Schmidt, and C. D'Emic, Microelectron. Eng. **59**, 341 (2001).
[25] E. P. Gusev, M. Copel, E. Cartier, D. A. Buchanan, H. F. Okorn-Schmidt, M. A. Gribelyuk, D. Falcon, R. Murphy, S. Mollis, I. Baumvol, C. Krug, M. Jussila, M. Tuominen, and S. Haukka, *Physical Characterization of Ultrathin Films of High Dielectric Constant Materials on Silicon*, in Physics and Chemistry of SiO_2 and Si/SiO_2 Interface, edited by H. Z. Massoud (ECS, Pennington, 2000).
[26] O. A. Aktsipetrov, A. A. Fedyanin, J. I. Dadap, and M. C. Downer, Laser Phys. **6**, 1142 (1996).
[27] J. I. Dadap, P. T. Wilson, M. H. Anderson, and M. C. Downer, Opt. Lett. **22**, 901 (1997).
[28] J. I. Dadap, B. Doris, Q. Deng, M. C. Downer, J. K. Lowell, and A. C. Diebold, Appl. Phys. Lett. **64**, 2139 (1994).
[29] S. T. Cundiff, W. H. Knox, F. H. Baumann, K. W. EvansLutterodt, M. T. Tang, M. L. Green, and H. M. vanDriel, Appl. Phys. Lett. **70**, 1414 (1997).
[30] J. E. Sipe, D. L. Moss, and H. M. van Driel, Phys. Rev. B **35**, 1129 (1987).
[31] W. K. Burns and N. Bloembergen, Phys. Rev. B **4**, 3437 (1971).

[32]J. L. Dawson, K. Krisch, K. W. Evans-Lutterodt, M. T. Tang, L. Manchanda, M. L. Green, D. Brasen, G. S. Higashi, and T. Boone, J. Appl. Phys. **77**, 4746 (1995).
[33]N. Shamir, J. G. Mihaychuk, H. M. van Driel, and H. J. Kreuzer, Phys. Rev. Lett. **82**, 359 (1999).
[34]M. L. Green, E. P. Gusev, R. Degrave, and E. Garfunkel, J. Appl. Phys. **90**, 2057 (2001).
[35]R. W. Kempf, P. T. Wilson, J. D. Canterbury, E. D. Mishina, O. A. Aktsipetrov, and M. C. Downer, Appl. Phys. B: Lasers Opt. **68**, 325 (1999).
[36]S. Zafar, A. Callegari, E. P. Gusev, and M. V. Fischetti, J. Appl. Phys. **93**, 9298 (2003).
[37]J. G. Mihaychuk N. Shamir, and H. M. van Driel, Phys. Rev. B **59**, 2164 (1999).